ELSEVIER
SAUNDERS

Clin Lab Med 27 (2007) 627–652

CLINICS IN
LABORATORY
MEDICINE

Rare-Event Analysis in Flow Cytometry

Albert D. Donnenberg, PhD*,
Vera S. Donnenberg, PhD

University of Pittsburgh School of Medicine, Hillman Cancer Research Center Suite2.42c, 5117 Center Avenue, Pittsburgh, PA 15213-2582, USA

Not everything that can be counted counts, and not everything that counts can be counted.

Albert Einstein (1879–1955)

Rare-event analysis is the art of finding a needle in a haystack, confirming that it really is a needle, and proceeding to make measurements to determine precisely what kind of needle it is. The frequency of the event of interest, and the signal-to-noise ratio of the method used to detect the event are the two most important factors.

Investigators who use the term, "rare-event analysis," usually are referring to detection of events that occur at a frequency of 1 in 1000 (0.1%) or less, although the record claimed in the literature has long stood at 1 in 10,000,000 (0.00001%) for tumor cells spiked into peripheral blood [1]. Detecting an event at low frequency requires a high signal-to-noise ratio and the acquisition of a large number of events. Technical aspects of rare-event detection have been reviewed in several articles [2–6] and are discussed here in a practical context, with two real-life examples.

A growing number of flow cytometry–based assays depend on rare-event detection. These include assays developed for basic science and for clinical applications. All of these assays were possible, but impractical, using conventional-speed flow analyzers (eg, Becton Dickinson FACSCalibur and Beckman Coulter Elite XL), which have maximum acquisition speed of 1000 to 3000 events per second. The high-speed analysis afforded by the most recent generation of cytometers and sorters makes the routine

This work was supported by grants BC044784 and BC032981 from the Department of Defense, a grant from the National Institutes of Health National Institute of Arthritis and Musculoskeletal and Skin Diseases (NO1 AR9 2239), and the generous support of the Hillman Foundation.

* Corresponding author.
E-mail address: donnenbergad@upmc.edu (A.D. Donnenberg).

0272-2712/07/$ - see front matter
doi:10.1016/j.cll.2007.05.013

acquisition of large data files practical for the first time, but in many cases this has only moved the bottleneck from data acquisition to data analysis. New software, taking advantage of parallel processing and the ability to address large blocks of random access memory directly, is on the horizon, removing the last obstacle to routine performance of rare-event assays.

A survey of rare-event applications

The major histocompatibility complex (MHC)/tetramer assay has been developed to detect peptide-specific T cells [7]. Peptides are presented to T cells in the context of PE or allophycocyanine (APC)-labeled self-MHC tetramers. Tetramers bind specifically to T cells having the appropriate receptor. MHC class I tetramers, which detect peptide-specific $CD8^+$ T cells, have been well characterized, whereas MHC class II tetramers, recognized by $CD4^+$ T cells, now are coming into use. Tetramer methodology is gaining popularity for study of infectious diseases, response to vaccines, tumor immunology, and basic immunology. Beckman Coulter Immunomics has commercialized tetramers for a variety of research applications. Tetramers that are not available commercially can be custom manufactured by the National Institutes of Health Tetramer Facility [8]. MHC allele protein production, folding, and quality control are free to approved investigators. Requestors incur the cost of peptide production and shipping. Reagents are quality controlled and are labeled by the facility with commercially manufactured streptavidin-allophycocyanin or streptavidin-phycoerythrin (PE) fluorophores.

Typically, 50,000 to more than 1 million events are acquired per sample, depending on the frequency of the cells specifically binding the antigenic epitope of interest. Samples usually are human peripheral blood; cell availability and cytometer/analysis time usually limit the application.

Analysis of rare T-cell subsets

These include antigen-specific cytokine secreting cells [9], in vivo apoptotic T cells [10], and analysis of V beta repertoire on T cells [11]. The latter has been commercialized by Beckman Coulter in a kit (IOTest Beta Mark) allowing simultaneous detection of three distinct V beta specificities using only two fluorescence parameters, fluorescein isothiocyanate [FITC] and PE. V beta detection has many research and clinical applications, including assessment of T-cell clonality. A recent Medline search on V beta and flow cytometry pulled up 204 citations.

Oncology

Detection of minimal residual disease and early relapse were among the first applications of rare-event technology. Large numbers of human peripheral blood leukocytes are assayed for one or more markers present on tumor

cells but absent in peripheral blood leukocytes. These include DNA ploidy [12], differentiation markers [13], and cytokeratin-positive/$CD45^-$ cells [14]. The same principle has been used in a Food and Drug Administration–licensed test, which first immunomagnetically preseparates circulating cells positive for an epithelial cell marker before detecting $CD45^-$ cytokeratin$^+$ cells by automated fluorescence microscopy [15,16]. The advent of more rapid and efficient rare-event analysis may allow such analyses to be performed in clinical laboratories by flow cytometry.

Cancer stem cells

The cancer stem cell paradigm has created quite a stir among cancer researchers, purporting as it does to identify the cancer-initiating cell [17] and the source of therapy-resistant recurrent disease [18–20]. Cancer stem cells are rare events within tumors, and candidate populations are characterized by the expression of a particular adhesion marker profile ($CD44^+$ $CD24^-$) [21]; the expression of CD133 [22], a marker first described on hematopoietic progenitor cells; the expression of the stem cell markers, CD90 and CD117 [19,20]; and multidrug resistance expression [19] and activity [20,23]. A rare-event problem par excellence, detection of cancer stem cells in disaggregated solid tumor samples, has to cope with the presence of cell clusters, dead cell, debris, autofluorescent cells, and the potential for tumors to harbor normal stem cells involved in wound healing and endothelial stem cells engaged in the generation of new blood vessels.

Hematopoietic stem cell research and transplantation

Applications in this rapidly growing field include quantification of side population (SP) cells, very early pluripotential hematopoietic progenitor cells present at extremely low frequency [24,25]; analysis of hematopoietic progenitor cell differentiation and phosphorylation [26]; and chemokine expression [27]. Quantification of hematopoietic progenitor cells in stem cell autografts, allografts, and in the blood of patients who have undergone stem cell mobilization is a routine clinical test, which has been commercialized by Beckman Coulter and Becton Dickinson. $CD34^+$ cells themselves are heterogeneous; quantification of the $CD34^+$ $CD38^-$ subset promises to provide a better clinical predictor of engraftment than measurement of total $CD34^+$ cells [28,29]. Because these subsets are rare, CD34 subsetting has not been adopted on a routine basis. The detection of microchimerism in the peripheral blood of solid organ transplant recipients also has potential for clinical research and clinical monitoring applications [30].

It also has been recognized that the bone marrow harbors rare endothelial [31] and mesenchymal [32] stem cells, both recognizable by their distinctive patterns of marker expression. Similarly, circulating endothelial cells are

proposed as a biomarker of vessel injury [33]. It is likely that flow cytometry also will prove increasingly useful for characterizing and isolating stem cells from solid tissues.

Detection of fetal cells in maternal blood

Prenatal diagnosis is facilitated by the detection of fetal cells in maternal blood [34–36]. This also is of interest to transplantation immunologists, because cells of fetal origin can be detected in the maternal circulation up to 27 years after pregnancy [37].

Detection of leukocytes in leukocyte-depleted platelet products

Platelet products routinely are leukocyte depleted to prevent spread of viral diseases, such as cytomegalovirus, to patients who are thrombocytopenic who also may be immunocompromised. Residual B cells can harbor latent Epstein-Barr virus [38]. Quantification of leukocytes in these components is critical to quality assessment [39], but the residual leukocyte count can be as low as 10 cells/mL of product. In the authors' laboratory, using a conventional-speed analyzer, it takes several hours to quantify and phenotype leukocytes in leukoreduced platelet components [40]. A commercially available in vitro diagnostic assay (LeucoCOUNT, Becton Dickinson), which detects the binding of propidium iodide to the DNA of nucleated cells but does not provide immunophenotypic information, can be performed in a few minutes per sample. The lower limit of detection of this assay, however, is in the range of 1000 cells/mL, according to the data provided on the package insert. Because the signal-to-noise ratio (discussed later) of propidium iodide–positive events is very high, the sensitivity of this assay could be increased tenfold simply by the application of high-speed cytometry.

Detection of cells injected or infused for biotherapy

Cellular therapy is an increasingly important research area with many opportunities for clinical application. In experimental models, therapeutic cells can be either transfected with the gene encoding a fluorescent protein marker, such as enhanced green fluorescent protein (EGFP), or marked with a tracking dye. Detection of these cells in the target tissue often is of critical importance. The authors have been able to detect DiD-labeled dendritic cells homing to the lymph nodes of rhesus macaques at a frequency of 1/38,000. The multiparameter analysis was performed at conventional speeds and required 20 to 30 minutes acquisition per tube [41]. Tracking dyes, such as carboxyfluorescein diacetate succinimidyl ester, not only allow detection of infused cells but also permit a reconstruction of their history of proliferation, because staining intensity decreases by half in each succeeding generation [42].

Dendritic cell biology

Dendritic cells and their precursors are present in peripheral blood at low frequency [43]. They play important roles in induction of immune responses to novel antigens and induction of tolerance. Quantification and subsetting of dendritic cells is of increasing interest in transplantation immunology [44,45], tumor immunology [46], autoimmunity [47], and infectious disease immunology [48].

Malaria diagnosis

Malaria can be diagnosed in the peripheral blood of immune patients by detecting rare circulating malaria pigment carrying monocytes [49]. To detect these cells, the investigators modified their fluorescence-activated cell sorter to measure depolarized side scatter as an additional parameter. Malaria pigment carrying monocytes were rare (1.5×10^{-4} to 8.8×10^{-4}) but formed a discrete population in plots of side scatter versus depolarized side scatter. Because the assay was performed on a cell sorter, the specificity of the assay for rare monocytes containing pigment granules was demonstrated by performing microscopy on sorted pigment positive cells.

Principles of rare-event analysis

Sample concentration and flow rate

Because the event frequency is an inherent property of the sample, there is not much to be done about it, save preprocessing the sample to enrich the event of interest. Immunomagnetic separation sometimes is performed before flow cytometry for this purpose [50]. This is preferable for rare-event isolation, because it can greatly decrease time required to sort a rare population on a fluorescence-activated cell sorter, but the uncertainties of event recovery after preseparation may obscure the true frequency of the event of interest. The advent of high-speed analysis obviates physical pre-enrichment, although the same principle is applied virtually. Cells are stained with a cocktail of linage markers, all labeled with the same fluorochrome. Cells expressing any of these markers logically are "gated out" of the analysis (discussed later). This technique also has the advantage of preserving the quantitative accuracy of the analysis, which is compromised when a physical pre-enrichment step is performed.

The frequency of the event of interest in the sample is one of the parameters that dictate how many total cells must be processed. The lower the frequency of the events of interest, the more events are necessary to acquire. The rate of sample acquisition can be manipulated in two ways: by concentrating the sample and by increasing the sample flow rate. Although it is tempting to shorten acquisition time by increasing the flow rate, this has its limitations. Analytic cytometers have variable flow rate settings that

correspond to the rate (microliters per minute) at which sample is drawn into the cytometer. An increase in the flow rate is accomplished by increasing the sample pressure relative to the sheath pressure. This results in a wider sample stream within the sheath fluid stream, increasing the opportunity for two cells to pass through the detection system at the same time (coincidence). It also increases the coefficient of variation of all of the measured parameters. Within the limits of the specifications of the cytometer used, it is better to maximize the event rate by optimizing the sample concentration. For example, if a cytometer draws sample at 1 microliter per second, the sample concentration (cells/mL) divided by 1000 is approximately equally to the sample acquisition rate in cells per second. In this example, concentrating the sample to 30×10^6 cells/mL yields a sample acquisition rate of 30,000 per second. Even high-speed cytometers, such as the Dako MoFlo and CyAn or Becton Dickinson FACSAria and LSRII, behave like conventional-speed instruments if the sample concentration is too low. Conversely, there is no advantage to concentrating the sample beyond the capacity of the instrument. At higher flow rates, it becomes important to gate out doublets using doublet discrimination (comparison of signal pulse height and width or area) (Fig. 1).

An alternate approach that can increase throughput and decrease data file size greatly is fluorescence threshold triggering, in which events below a certain threshold of fluorescence are not seen by the cytometer and, therefore, not collected as events. This method requires that the rare event be very brightly labeled and that the denominator (number of cells processed) be inferred from the sample flow rate [51].

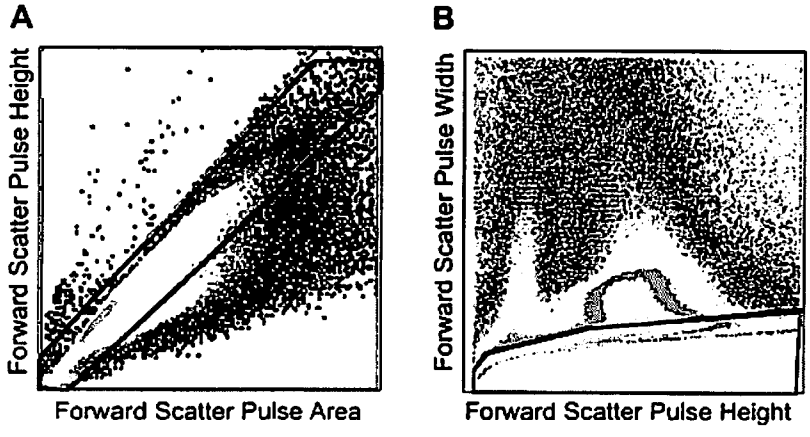

Fig. 1. Doublet discrimination can be performed by comparing pulse analysis parameters. The pulse parameters used for doublet discrimination differ between cytometer manufacturers. The data in panel A were collected using a Beckman Coulter FC500 cytometer, where forward light scatter pulse area (X axis) is compared with forward light scatter pulse height. A cell doublet (or multicellular cluster) is an event with a pulse height too small for its area. The data in panel B were collected on a Dako CyAn, where forward light scatter pulse height (X axis) is plotted against forward scatter pulse width. A cell cluster has a width too large for its peak. In both histograms, singlets are shown within the polygonal regions.

Signal-to-noise ratio

The signal-to-noise ratio sets an absolute limit on the lowest frequency of events that can be detected before they are overwhelmed by background. The critical task of enhancing the signal-to-noise ratio may be approached from the standpoint of minimizing noise and maximizing signal. Noise is defined as anything that creates spurious signals that can be confused with the signals (fluorescence or light scatter) used to define the event of interest. Noise can result from nonspecific binding of a fluorescent probe, the presence of autofluorescent biomolecules, the presence of coincident events or cell clusters, or sporadic mechanical or electrical perturbations (including sample carryover). Dead or dying cells are particularly bad actors. The techniques to minimize these factors and to maximize signal are discussed later.

Two important factors bear on the signal-to-noise ratio: the difference in fluorescence intensity between negative and positive populations and the dispersion of these two populations (usually expressed as their coefficients of variation). Some membrane dyes give very bright homogeneous signals and, therefore, place cells far from noise. When using combinations of fluorochrome-conjugated antibodies, the authors often reserve PE for the most critical measurement, because the excitation and emissions spectra are widely separated and the extinction coefficient and quantum yield are high compared with other commonly available fluorochromes [52]. Fig. 2 illustrates the detection of CD8 on peripheral blood lymphocytes using eight different fluorochromes where signal-to-noise ratios ranged from 18 (Cascade Yellow excited by a 405-nm violet laser) to 1367 (PE-Cy5 excited by a 488-nm blue laser). In Fig. 2, signal to noise was calculated as a simple ratio of geometric mean fluorescence intensity in the $CD8^+$ population divided by that of the negative population. An alternative means of looking at signal versus noise is the mean channel separation, which is calculated by taking the difference of fluorescence intensities divided by a pooled SD of both populations. This latter method has the advantage of taking into account the spread of the negative and positive populations.

Tagging cells with antibodies conjugated to brightly labeled fluorescent immunobeads also can result in a significant increase in signal-to-noise ratio compared with immunofluorescent staining. This method has been used to detect fetal red blood cells in the maternal circulation at a frequency of 1 per 100,000 [53].

When autofluorescent myeloid cells, cellular debris, or red blood cells interfere with rare-event detection, it often is possible to move them out of the way by targeting them with a specific antibody. For example, Owens and Loken used CD14 to move monocytes and granulocytes away from $CD34^+$ progenitor cells [54]. The authors have used a similar strategy to perform functional assays on dendritic cells that comprise a small proportion of bronchoalveolar lavage cells [6].

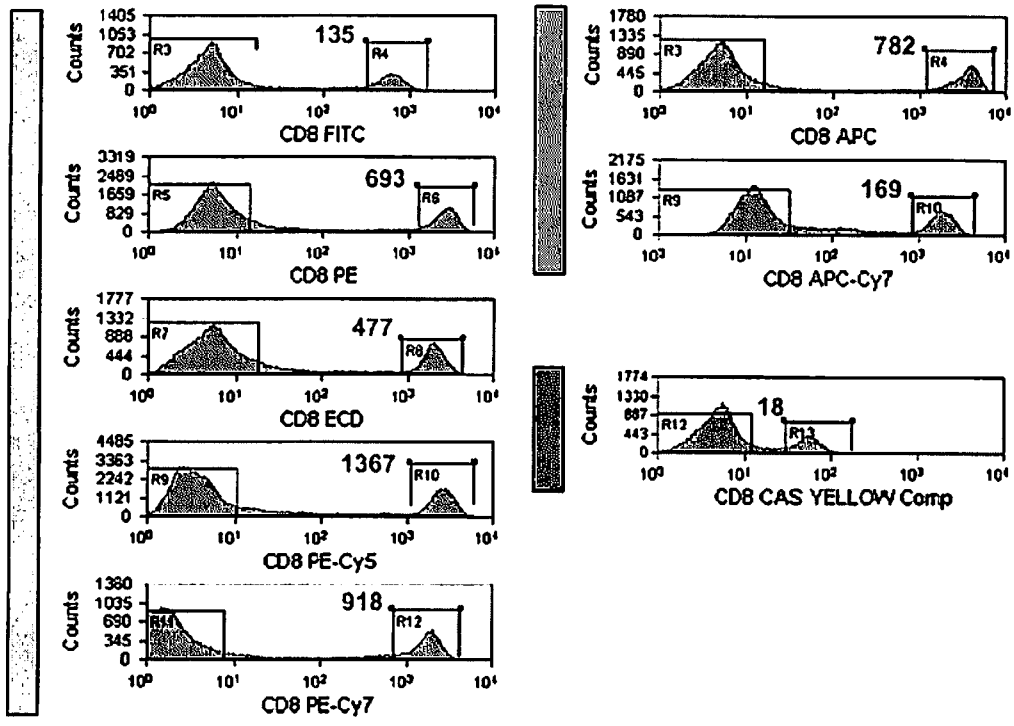

Fig. 2. Signal-to-noise ratio in the detection of CD8 on peripheral blood lymphocytes using eight different fluorochromes. Isolated peripheral blood mononuclear cells were stained with directly conjugated antibodies to the surface determinant CD8 and acquired during the same session. FITC, PE, and the PE tandem dyes were excited with a 488 diode laser; APC and APC-Cy7 were excited with a 635-nm diode laser; and Cascade Yellow was excited with a 405-nm violet diode laser. With the exception of the Cascade Yellow conjugated antibody, which was a custom conjugate, all antibodies were purchased from commercial sources. Signal-to-noise was calculated as the geometric mean fluorescence of the CD8+ cells, divided by the geometric mean fluorescence of the $CD8^-$ cells. Because some of the antibodies represent different clones (and may be reactive to different epitopes), these data do not provide a pure comparison of the signal-to-noise characteristic of the fluorochromes and negative cells alone. Signal to noise also is dependent on other factors, such as antibody avidity and concentration and fluorescence-to-protein ratio.

Another important aspect of the overall signal to noise is the number of parameters used to define the rare event of interest. Modern multilaser, multi–photomultiplier tube instruments permit detection strategies that make use of multiple parameters to define the rare event. As described previously, the rare event of interest should be identified positively by more than one fluorescence parameter. Not quite as obvious is the importance of including at least one fluorescence parameter for which the rare event is negative. In rare-event detection, it is almost as important to specify where the rare event is not, as to specify where it is. In some experimental settings, it is possible to obtain a positive control sample in which the event of interest is not rare. This is helpful especially for defining a set of compound logical gates that assign the population of interest a unique location in multiparameter space. Compound gating strategies that maximize detection

of events in the positive control while minimizing false-positive events in the negative control can be determined empirically and applied to the experimental data. Such analyses are performed after the fact, on listmode data files. Using these principles, Gross and colleagues [1] were able to detect a breast carcinoma cell line spiked into peripheral blood at a frequency of 1 cell per 10,000,000. This rivals the sensitivity of the polymerase chain reaction assay and seems to be the current world record for rare-event detection by flow cytometry.

Cellular autofluorescence can interfere greatly with rare-event detection, primarily because of the presence of native fluorescent intracellular molecules, such as flavins [55], which are excited by blue-green light (the 488 line provided by argon lasers) and emit over a broad range of wavelengths. Autofluorescence often presents a problem in cultured cells but also may be encountered in disaggregated freshly isolated tissues. As long as the rare event of interest itself is not highly autofluorescent, autofluorescent cells can be eliminated from the analysis by acquiring an unstained fluorescence parameter in the range of the autofluorescence (usually confined to the emission ranges of FITC through Texas Red dyes) or by staining with an antibody conjugated to a dye in the range of wavelengths that is known not to react with the rare event of interest. Cells positive for this parameter can be eliminated logically during analysis with a *not* gate (Fig. 3) [56]. A fluorescence channel reserved for the elimination of autofluorescent cells or other bad actors is known as a dump parameter.

Autofluorescence also can be reduced or eliminated using a laser line longer than the wavelength that excites autofluorescent intracellular molecules [57]. Some commercially available cytometers (BD FACSArray and Cytonome) use a green laser line (eg, 531 nm) to minimize excitation of flavinoids while providing more efficient excitation of PE and the PE tandem dyes.

Dead and dying cells are present in cultured cells and disaggregated solid tissues and often are noisier than live healthy cells. They can be eliminated from the analysis of rare events by a variety of techniques using logical gates. Low light scatter events (compared with resting lymphocytes) and events on the low side of lymphoid forward scatter with higher side scatter typically represent subcellular debris and late apoptotic cells, respectively. They can be eliminated most effectively after creating a positive gate on a population of interest (Fig. 4). If an instrument is equipped with an ultraviolet or violet laser, advantage can be taken of the properties of 4'-6-diamidino-2-phenylindole (DAPI), a DNA intercalating stain. Live cells are impermeant to DAPI; thus, DAPI-excluding cells are live and $DAPI^+$ dead cells can be removed by gating. For cells that have been stained, fixed, and gently permeabilized (eg, with saponin), DAPI can be used to measure DNA content in all cells (Fig. 5). Erythrocytes, subcellular debris, and apoptotic cells can be identified easily as being hypodiploid and removed by gating. Other DNA intercalating dyes (7-aminoactinomycin D and propidium iodide) that are excitable with a blue laser can be added to stained

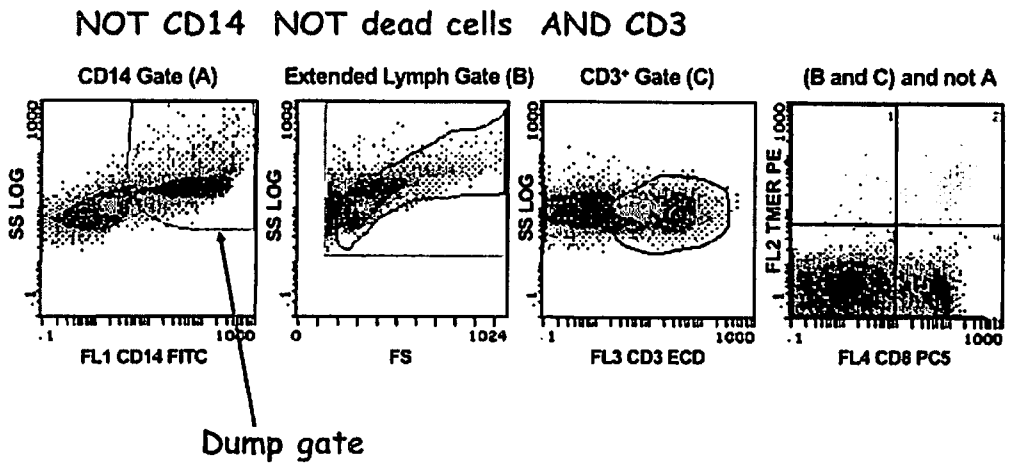

Fig. 3. Use of a dump gate to remove spurious signals. Measuring the tetramer response of a healthy $A2^+$ control subject to influenza tetramer (peptide GILGFVFTL) requires a compound gating strategy in which $CD14^+$ cells are eliminated using a dump gate (*A*). Apoptotic, dead cells and debris are eliminated with a light scatter gate (*B*) and $CD3^+$ cells are selected, before visualizing anti-CD8 versus tetramer binding. Removing cells positive in FL1 (FITC-conjugated anti-CD14) by NOT gating eliminates monocytes, a potential source of nonspecific tetramer binding, from the analysis. It also eliminates any events that are positive in the FL1 channel by reason of autofluorescence. These events also would be positive in the FL2 (PE) channel and, thus, be confounded with genuine tetramer-binding events. The $tetramer^+$ events are color evented in red. (*Modified from* Hoffmann TK, Donnenberg VS, Friebe-Hoffmann U, et al. Rapid communication: competition of peptide-MHC class I tetrameric complexes with anti-CD3 provides evidence for specificity of peptide binding to the tcr complex. Cytometry 2000;41:321–8.)

unfixed cells before acquisition. Dead cells permeant to these dyes can be recognized and gated out by their broad emissions spectra (typically spanning several fluorescence parameters) and bright staining. Thus, dead cells identified by these dyes usually can be distinguished from live cells stained with fluorochromes having overlapping emission spectra.

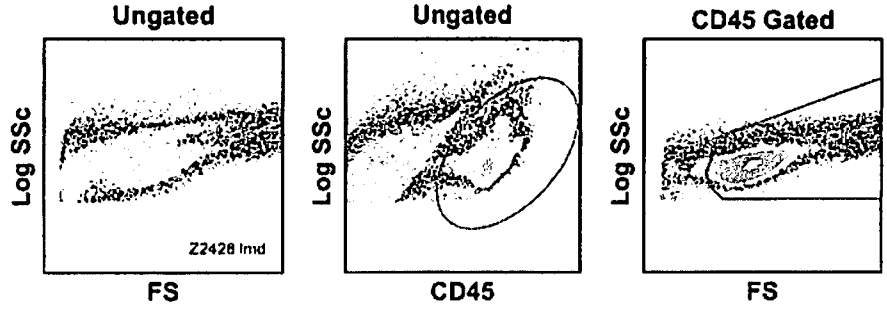

Fig. 4. Elimination of low light scatter debris often is performed best after identifying a population of interest by antibody staining and side scatter. It might be difficult to discriminate between debris and hematopoietic cells in the ungated histogram on the left, but after focusing on the events of interest $CD45^+$ cells (*center*), this becomes a much easier task (*right*).

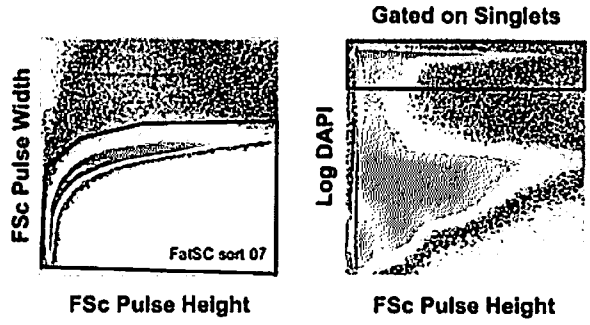

Fig. 5. A very messy sample is cleaned up before analysis by doublet discrimination followed by DAPI staining. The sample is the stromal vascular fraction of human fat, obtained after collagenase digestion, mechanical disaggregation, and centrifugation. Doublet discrimination was performed as described in Fig. 1. The cells were stained, fixed, and permeabilized. Prior to analysis, the ultraviolet/violet-excited DNA intercalating dye DAPI was added. Log DAPI fluorescence intensity was collected to emphasize the difference between hypodiploid cells and debris and cells diploid or greater DNA (rectangular region).

The time parameter, which can be saved as a listmode parameter or calculated offline, also can help recognize and eliminate noise encountered during long sample acquisitions. Plotting a single parameter (eg, forward scatter) as a function of time facilitates the identification of event bursts caused by minor clogs or other transient problems (Fig. 6). Another familiar problem that can be eliminated using the time parameter is the flurry of spurious events that occurs when a sample tube is allowed to run dry and air is aspirated. These deviations can be recognized and removed from the analysis with a logical gate. Alternatively, event bursts can be identified as deviations from an expected Poisson distribution. Custom software has been designed to detect such deviations and filter them out for rare-event analysis [58].

One important aspect is to characterize the total noise using an appropriate negative control. Sometimes it is possible to devise a control sample that is identical to the experimental sample in all respects, except that it does not

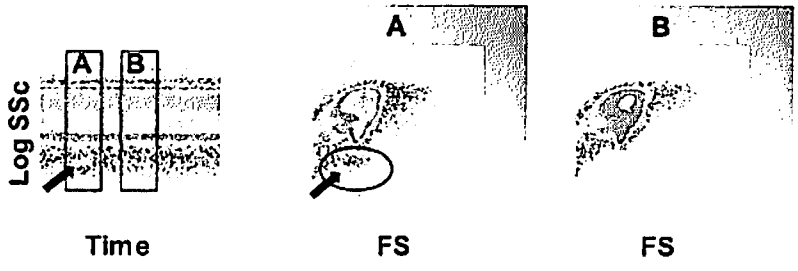

Fig. 6. Identification of a burst of spurious events using the time parameter. A plot of log side scatter versus time reveals the transient appearance of a low side scatter population (*A, arrow*). These events can be visualized more clearly (*arrow, elliptical region center histogram*) by comparing side versus forward scatter on this time segment and a comparable segment (*B*).

contain the rare event of interest (eg, peripheral blood from a non-MHC A2 individual in an MHC A2 tetramer-binding assay or blood from a cancer-free normal subject in a circulating cancer cell assay). In other cases, it may be necessary to resort to control reagents, such as isotype-matched fluorochrome-conjugated antibodies. In the latter case, a few caveats apply: the control reagent must be similar to the experimental reagent with respect to the ratio of fluorescent dye to protein (for commercial reagents, this is seldom on the package insert but sometimes this can be determined by a call to the vendor), and it must be used at the same concentration. Additionally, staining must be designed so that the same gating strategy used to detect the rare event can be applied to the negative control sample. Roederer [59] has called this the fluorescence minus one approach. As an example, consider detection of $CD34^+$ cells (hematopoietic progenitor cells) in peripheral blood using the two-color combination and anti-CD45 FITC and anti-CD34 PE. $CD34^+$ progenitor cells have characteristic light scatter and CD45 expression but relatively dim CD34 expression. Thus, when $CD34^+$ cells are present at low frequency, they can be difficult to detect. The analytic strategy used to pull them away from noise is to first create a gate based on side scatter and CD45 expression [60]. This gate contains the $CD34^+$ cells (still a rare population among mostly lymphoid cells) but excludes myeloid cells that interfere with CD34 detection because of autofluorescence and nonspecific antibody binding. If two irrelevant isotype-matched conjugated antibodies (eg, IgG_1-FITC plus IgG_1-PE) were used as a negative control, it would be impossible to duplicate the gating strategy used to identify the population in which $CD34^+$ progenitor cells were identified (ie, cells with intermediate CD45 expression and low side scatter). Thus, the appropriate negative control is anti-CD45 FITC plus IgG_1-PE or plus anti-CD34 PE admixed with a great excess of unlabeled anti-CD34. Beckman Coulter has used the latter strategy in their commercial CD34 enumeration kit. Using either of these controls, the amount of total noise in the system, hence the limits of sensitivity of the assay, can be determined by looking at the frequency of spuriously positive events (IgG_1-PE positive) within the same CD45-scatter gate used to identify the $CD34^+$ cells. In this context, an identical number of events must be acquired for the negative control sample as for the experimental sample. Resist the temptation to acquire fewer events because there is nothing there. If the frequency of spuriously positive events is 0.02% (1 in 5000), it is impossible to use this assay to detect $CD34^+$ cells present at a frequency of 1 in 10,000, no matter how many events are acquired! Thus, the frequency of false-positive events (noise) determines the lower limit of detection. It follows that there is a point of diminishing return beyond which acquiring a greater number of events increases the precision of the rare event frequency estimate but does not increase the sensitivity of the assay.

After determining the lower limit of detection, the optimal number of cells to be acquired routinely can be determined empirically for a given

assay. This can be done by acquiring a large number of cells on samples from a series of subjects. Each data file can be gated into segments containing different numbers of cells based on time or event count parameters. Fig. 7 illustrates an example in which the listmode file from a CD34 determination, consisting of 1,300,000 events, was sampled 9 times (5000 to 400,000 cells per sample) by creating triplicate gates on the a histogram of time by forward scatter. The coefficient of variation associated with each triplicate was calculated and plotted as a function of the number of cells sampled (Fig. 8). Sampling data from a large file simulates acquiring many individual replicate samples. Acquiring 5000 cells gave a coefficient of variation of 50%, too imprecise for a reliable assay. The coefficient of variation decreased as a function of the number of cells assayed and seems

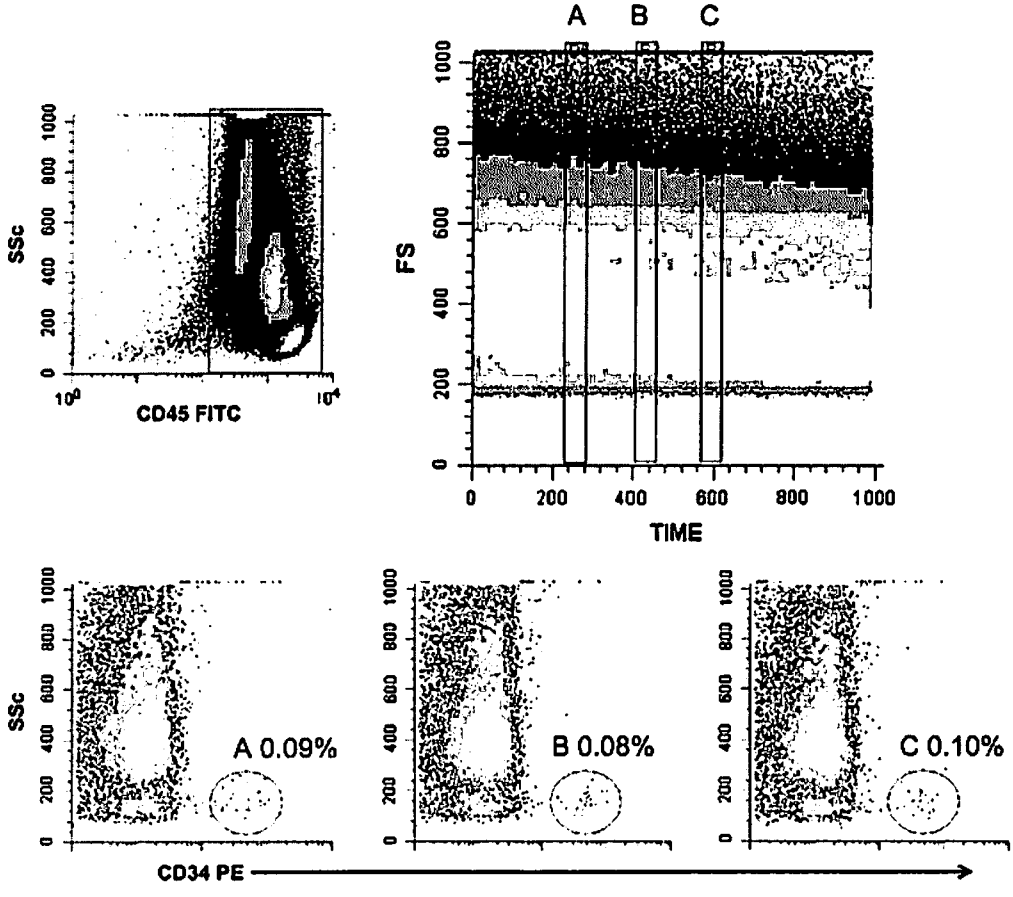

Fig. 7. Replicate sampling of a data file using the time parameter. Peripheral blood cells were stained with antibodies against CD45 and CD34. A total of 1,300,000 events was acquired into a listmode data file. The upper-left histogram was used to gate out a small proportion of CD45-negative events. The upper-right histogram (forward scatter by time) was used to create three gates of equal size (A, B, C), including approximately 80,000 cells each. The lower histograms identify $CD34^+$ side scatter low cells. The replicate determinations were used to calculate a coefficient of variation (SD divided by the mean). The process was repeated 9 times with gates of varying size. The results are plotted in Fig. 8.

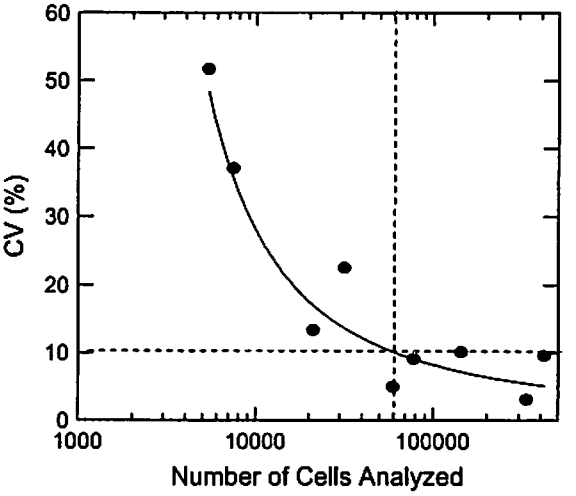

Fig. 8. Empiric determination of the optimal number of cells to acquire for analysis of $CD34^+$ cells. A large number of events (1,380,845) was acquired to a single listmode data file using a standard CD34 assay (StemKit, Beckman Coulter). A sample known to have a low CD34 frequency (0.1% of $CD45^+$ cells) was chosen. $CD34^+$ events were defined as $CD45^+/CD34^+$ events with low side scatter. To sample different segments of the data file repeatedly, forward scatter was plotted versus time. The analysis of percent $CD34^+$ was performed, gating on increasing numbers of cells (5000 to 400,000). For each number of cells, the analysis was performed in triplicate. The coefficient of variation (CV) (ratio of the SD to the mean percent $CD34^+$) was plotted versus the number of cells analyzed. A power curve smooth ($y = ax - b$) was fitted though the data. A CV of 10% was achieved when approximately 60,000 cells per replicate were analyzed (*dashed lines*).

to have approached a lower limit of approximately 5%. Interpolating from a power curve fit to the data, an acceptable coefficient of variation of 10% was achieved when 60,000 cells were analyzed. In practice, the authors' clinical laboratory routinely acquires 75,000 cells from each of duplicate samples stained for CD34 enumeration.

Reproducibility

The results of successful rare-event analysis often visually are unimpressive. Against a denominator of a million or more acquired events, there is a small number of positive events that have been filtered through a series of gates defining the population of interest. Sometimes the events form a tight cluster in a 2-parameter scatterplot. Sometimes they seem diffuse in 2-parameter space but are unique in multiparameter space. The credibility of such determinations can be enhanced greatly by performing replicate determinations. During assay development, the authors routinely stain three independent samples, acquiring the same number of events for each. Thus, the frequency of rare events can be reported as the mean and the associated CI. The frequency of false-positive events detected in the negative control sample (also collected in triplicate with the same number of events

as the experimental sample) also is reported, and a lower limit of detection calculated as the upper 99th percentile of negative control is interpreted as the lower limit of detection [56]. If replicate samples cannot be acquired, a gating method similar to that used for Fig. 7 can be used to divide the file into three equal time segments. These segments then are analyzed separately, and the mean and SD determined. This method accounts for any inhomogeneity in the data file resulting from sampling or instrument performance, but unlike running three independent samples, it does not account for variability resulting from sample preparation.

Specialized analytic software

The emergence of rare-event detection as an increasingly important application of flow cytometry has left somewhat of a software gap. Throughout this article, examples are presented in which data files consisting of 5 to 14 parameters measured on as many as 10 million events have been analyzed. Until recently, this could have been a painful procedure, owing to the fact that neither the native software supplied with cytometers nor aftermarket offline analysis products have been designed to analyze large data files. To cite a particularly egregious example, the authors transported their fastest workstation, dual monitors, and an external hard drive to a cottage in the Allegheny Mountains to complete the analysis of a languishing dataset during a family vacation. The dataset consisted of approximately 50 eight-color data files of 250,000 to 2.5 million events each, identifying stem cell marker–positive cells among rare solid tumor cells expressing the multiple drug resistance transporter, ABCG2 [19]. The authors honored their resolution to rise early and work without interruption until noon every day during the 10-day holiday. Braving inexplicable software crashes sending them back to square one, excruciating refresh intervals each time a region or a gate was adjusted, and all manner of additional indignities, the analysis was barely completed in the allotted time.

This story was related to Microsoft, which wished to publicize the development internally, by Applied Cytometry Systems of Sheffield, United Kingdom, of a new generation of flow cytometry software that makes efficient use of scalable parallel processing and Microsoft's new 64-bit XP and Vista operating systems. The authors have the new software, dubbed Venturi, now nearing commercial release, running eight simultaneous hyperthreads on a dual-core, dual-processor 64-bit workstation. In addition to a conventional data analysis space in which histograms, logical gates, and analytic regions are created, the software provides a preview matrix of all possible one- and two-parameter histograms. This preview can be focused on populations defined by any gate created within the analysis space. A double click on any graph on the preview page copies it to the analysis space, where regions and other analysis tools can be applied. This provides an unprecedented opportunity for data exploration. Because of the extensive use

of directly addressable random access memory and the efficient division of data calculations and display into parallel processes, complex analyses of large data files can be performed with unprecedented speed and less mental anguish. It is likely that Venturi will set a new standard for the analysis of large data files. By way of disclosure, the authors have a collaborative relationship with Applied Cytometry Systems but serve as unpaid consultants without financial interest in the company.

Statistical analysis of rare-event datasets

Data analysis almost always involves the comparison of groups of data. The most common and powerful tests of statistical confirmatory analysis, such as the Student *t* test and linear regression analysis, assume that the data are distributed normally. Normally distributed data are symmetric and bell shaped. The mean gives the center of the distribution and the SD describes the spread. When a test, such as the Student *t* test, is used to compare data from two groups, only three parameters are used in the test: the mean values of the two groups and a pooled estimate of the SD. If these parameters describe the dataset well, tests assuming normality are appropriate. The Student *t* test is what is known as a robust test. This means that the data need not fit the normal distribution perfectly in order for the test to be valid. This said, most rare-event data are log-normally distributed and require transformation before statistical analysis. Applying the Student *t* test to raw rare-event data almost always results in overestimation of the mean values (because of the skewness of the distribution) and overestimation of the SD, resulting in a loss of statistical power. Several tools exist to check a dataset for normality; the most common is the normal probability plot (Fig. 9). Raw and log-transformed data can be plotted. The plot showing the most linear relationship between observed results and results predicted by the normal model help choosing between analyzing raw or transformed data.

Rare-event detection: two examples

Detection of cells expressing stem cell markers in normal human lung tissue

Performing rare-event flow cytometry on cells from solid organs presents several challenges. Tissue fragments must be digested and disaggregated mechanically before staining. Even the most meticulous preparation leaves cell clusters, dead cells, and cellular debris, all of which can interfere with analysis. In this example, human lung tissue was minced using a Becton Dickinson Medimachine, filtered though a 70-μ cell strainer, digested with collagenase, and separated on a Ficoll-Hypaque gradient. The resulting single cell suspension was stained with the following antibodies: CD90-ECD, ABCG2-PC5, CD117-PC7, CD133 APC, and CD45-APCC7; fixed;

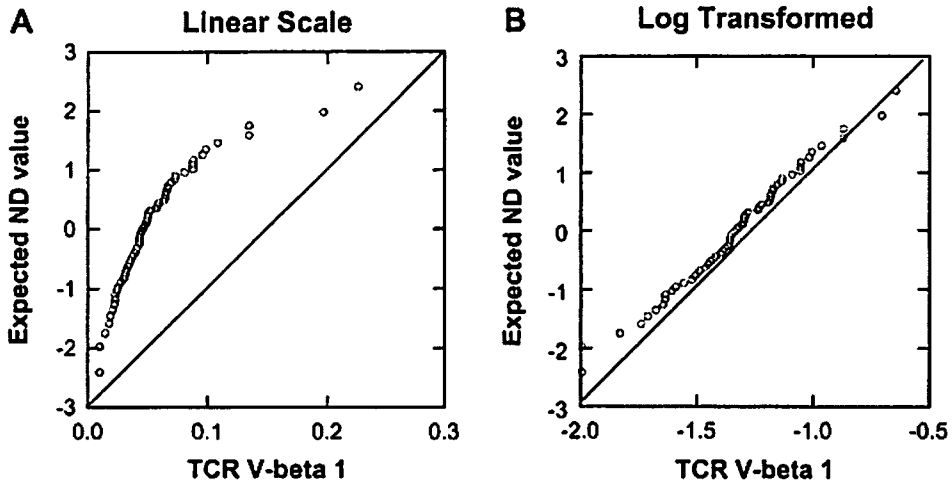

Fig. 9. The distribution of T-cell receptor V beta expression 1 on peripheral blood T cells is log-normally distributed. The normal probability plot provides a useful and commonly available tool for evaluating data distributions. Here, the ordered data (X axis) are plotted against the value predicted by the normal distribution (normalized to a mean of 0 and a SD of 1). A linear relationship indicates that the data are well described by the normal distribution and is evidence of the appropriateness of using tests requiring normality. The distribution of V beta 1 is shown for a group of both raw (*A*) and log-transformed (*B*) results. The probability plots clearly demonstrate that V beta usage is modeled more closely by the normal distribution after log transformation.

permeabilized with saponin; and stained with anti-cytokeratin FITC and anti-p53 PE. Immediately before acquisition, the DNA stain DAPI was added. A total of 2.4 million events was acquired using a Dako CyAn cytometer. Spectral compensation and data analysis were performed on the listmode data file using Venturi software (Applied Cytometry Systems).

Analysis of the multiparameter data was performed in four steps: (1) data cleanup, (2) gating on the populations of interest (classifier populations), (3) detection of outcome parameters on populations of interest, and (4) exploring the relationship between classification parameters and outcome parameters through color eventing. As described previously, elimination of cell clusters by doublet discrimination (see Fig. 1), small debris by forward and side scatter (see Fig. 3), and elimination of hypodiploid cells and debris with DAPI (see Fig. 5) all were used to clean up this lung tissue sample (Fig. 10) before defining two classifier populations: $CD45^-$ cells having simple versus complex morphology, as determined by side scatter. The rationale for this dichotomy comes from the hypothesis that tissue stem cells are stem cell marker–positive cells with simple morphology (small cells with high nucleus to cytoplasm ratio and, therefore, low forward and side scatter), progenitor cells are stem cell marker–positive cells with complex morphology (reflecting their more active state), and mature cells are stem cell marker–negative cells of complex morphology.

Having defined the classifier populations, it is now possible to examine expression of the outcome parameters, in this case the epithelial differentiation

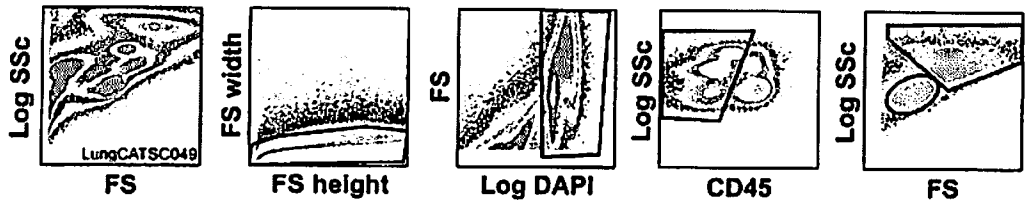

Fig. 10. Gating strategy for multiparameter analysis of stem cell marker–positive cells in disaggregated human lung tissue. Doublet discrimination, DAPI staining, and light scatter properties were used for data cleanup, eliminating cell clusters, hypodiploid cells, and subcellular debris. After cleanup, CD45 and side scatter were used to define hematopoietic ($CD45^+$) and nonhematopoietic populations. Light scatter properties were used to divide the CD45-negative population further into cells with simple versus complex morphology. The two classifier populations carried forward for analysis of outcomes (see Fig. 11) are CD45-negative cells simple morphology and $CD4^-$ cells of complex morphology.

marker, cytokeratin; the stem/progenitor markers, CD90, CD117, and CD133; the cell cycle (and tumor suppressor) protein, p53; and the multiple drug resistance transporter, ABCG2. The relationship between classifier and outcome parameters is a fluid one, which may change after exploratory analysis. This relationship also is highly dependent on the extent of the available pre-existing information concerning the cell populations and markers of interest. To choose a straightforward example, in the analysis of activated T-cell cytokine production, T-cell subset markers clearly constitute the classifiers, and antibodies identifying specific cytokines are the outcomes. Exploratory analysis also may lead to including light scatter properties among the outcome variables, if these change on induction of cytokine production. To return to the example, because there is little to no pre-existing information concerning the markers of interest on human lung stem cells, the outcomes analysis first focuses on co-expression of the differentiation marker, cytokeratin, in relation to the other outcome parameters (Fig. 11). More insight can be gained into the complex relationship between these markers and the outcome variable through the use of color eventing. Putative stem cells (cells expressing any stem cell marker [CD90, CD117, or CD133] and having simple morphology) were color-evented cyan; progenitor cells (cells expressing any stem cell marker and having complex morphology) were color-evented magenta. Mature cells (stem cell marker–negative) are color-evented black. Clearly, dim expression of CD90 is the predominant marker on this cytokeratin-negative putative stem cell, followed by CD133. Bright CD90, bright CD117, and the majority of CD133 expression occurs on cytokeratin dim cells of complex morphology (candidate progenitor cells). Dim expression of all stem cell markers also extends to a discrete population of cytokeratin bright cells. The bulk of simple and complex cells do not express stem cell markers. The transporter ABCG2 is most prevalent on the putative stem cells but has its highest expression on cytokeratin dim progenitor cells. The expression of p53 resembles that of ABCG2. Although this analysis provides a good starting

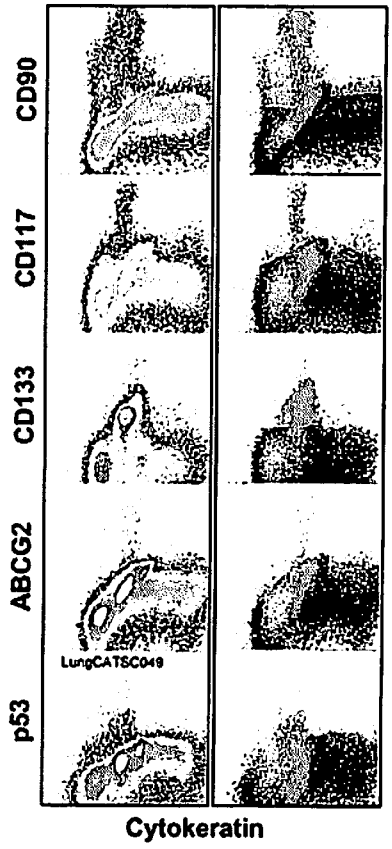

Fig. 11. Use of density histograms and color-evented dot plot to evaluate classifier variables in the context of outcome variables. Candidate stem and progenitor populations are color-evented cyan and magenta, respectively, with cyan having color precedence.

place, a further area of investigation is the relationships among the outcome variables.

Polychromatic flow cytometry for simultaneous phenotypic and functional analysis of antigen-specific T cells

Rare-event detection can be combined with functional analysis. This example took advantage of a prototype 12-color, 4-laser cytometer (Beckman Coulter) to evaluate the effect of MHC-tetramer binding on calcium flux in subsets of $CD8^+$ T cells. For this demonstration, peripheral blood mononuclear cells were obtained from a healthy HLA $A2.01^+$ subject who had a known high frequency of cytomegalovirus (CMV) tetramer-binding cells. Cells were stained with antibodies directed against cell surface markers (Table 1) and maintained at 37°C during sample acquisition in the presence of the calcium sensitive dye, Indo-1 [61]. Fig. 12 shows the effect of addition of the APC-conjugated CMV-pp65 tetramer, NLVPMVATV, directly to the cells during acquisition. $CD4^+$ and $CD8^+$ cells became brighter in APC immediately after tetramer addition, indicating the level of nonspecific binding,

Table 1
Lasers, fluorochromes, and antibodies used for 12-color analysis (Figs. 11–15)

UV (355)		Violet (408)		Blue (488)	
FL9	FL10	FL11	F12	FL1	FL2
(Indo short)	(Indo long)	Pacific Blue	Cascade Yellow	FITC	PE
Indo	Indo	C1.7	CD45	CD7	CD95

This panel was used for the data collected in Figures 11 through 15.

but CD8$^+$ cells developed a unique APC bright population indicative of tetramer binding. This dual staining (dim nonspecific and bright specific) is not seen when unbound tetramer is removed after staining by washing.

Fig. 13 shows the kinetics of calcium flux on CD8 tetramer$^+$, CD8 tetramer-negative, and CD4$^+$ populations after the addition of (1) tetramer; (2) the CXCR4 ligand, SDF1; and (3) the calcium ionophore, ionomycin. Fig. 14 shows that same data subjected to a running median curve-smoothing algorithm. To accomplish this, the gated listmode data were exported from WinList into a statistical package (Systat 11, Systat Software, San Jose, California). Calcium flux occurred on tetramer$^+$ CD8$^+$ cells concomitant to tetramer binding. A slight and gradual increase in intracellular

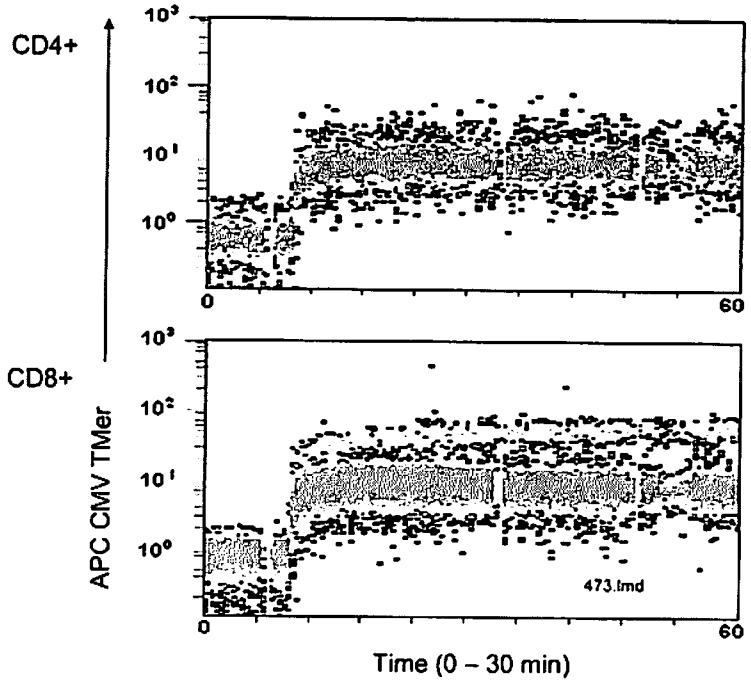

Fig. 12. Peripheral blood cells mononuclear from a CMV-seropositive HLA A2$^+$ subject were stained as described in Table 1 and held at 37°C during sample acquisition. After approximately 4 minutes, acquisition was interrupted momentarily and the CMV tetramer, NLVPMVATV, was added. Addition of the tetramer resulted in a marked elevation of background fluorescence in CD4$^+$ and CD8$^+$ T cells, but a tetramer$^+$ population, apparent immediately on tetramer addition, emerged as a distinct population among CD8$^+$ cells after approximately 15 minutes.

			Red (635)		
FL3	FL4	FL5	FL6	FL7	FL8
PE-Texas Red	PE-Cy5.5	PE-Cy7	APC	APC-Cy5.5	APC-Cy7
CD45RA	CD8	CD8β	TMER	CD27	CD28

calcium concentration was seen in all populations on addition of SDF1, and robust calcium flux was seen in all populations within 2 minutes of the addition of ionomycin.

The authors used a classifier/outcome strategy to explore the identity of tetramer$^+$ cells and cells evidencing high calcium flux. Classifiers can be hierarchic. In this case, the primary classifiers used for cleanup and to define CD8$^+$ T cells were CD45$^+$, forward and side light scatter lymphoid gate, and CD8 plus CD8 beta double positive. Subsets were defined within CD8$^+$ cells using CD45RA versus CD27, CD45RA versus CD28, CD7 versus C1.7, and CD95 versus CD45RA as secondary classifiers (Fig. 15). Unlike the example in Fig. 11, where color eventing was used to highlight

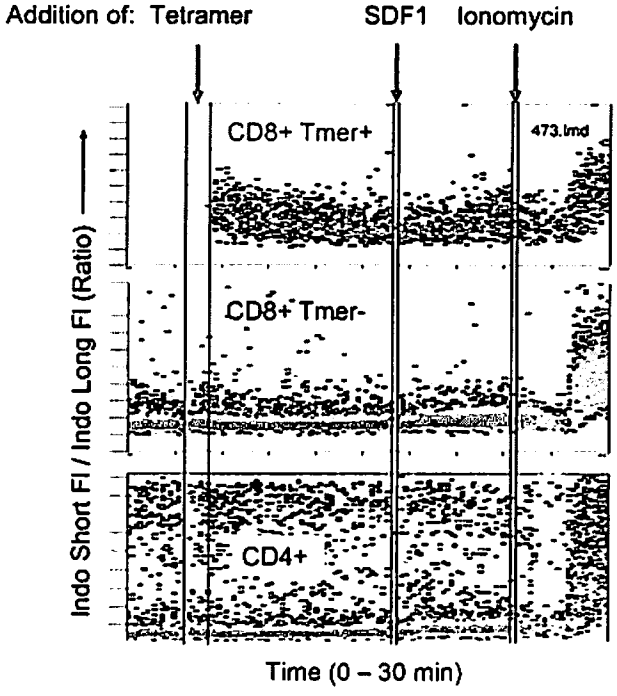

Fig. 13. Kinetics of calcium flux in CMV tetramer-positive and -negative CD8$^+$ T cells and CD4$^+$ T cells. Calcium flux is detected as an increase the ratio of Indo short fluorescence to Indo long fluorescence. With some imagination, an increase in intracellular concentration can be seen in tetramer-positive cells immediately after tetramer addition. It is difficult to discern a response to SDF1 in any population, and all populations clearly responded to the addition of ionomycin.

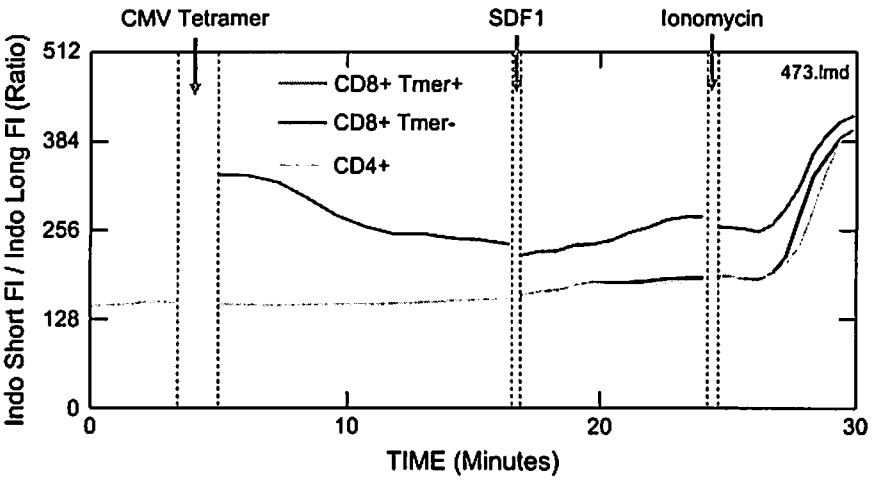

Fig. 14. A running median curve-smoothing algorithm provides a means of visualizing subtle changes in intracellular calcium flux. The kinetics of rise and decay of intracellular calcium levels is apparent in tetramer-positive $CD8^+$ cells. The curve smoothing also eliminated any apparent differences between $CD8^+$ tetramer-negative cells and $CD4^+$ cells. The gradual effect of SDF1 clearly is visible in all populations, as is the immediate effect of ionomycin.

classifier populations on outcomes, colors were used to highlight outcomes (tetramer$^+$, high calcium flux after addition of tetramer) on the very complex set of potential classifiers. The color-evented populations clustered in multiparameter space with respect to virtually all of the classifiers, with tetramer$^+$ and high calcium flux cells largely concordant. This is of interest, because they fall somewhere between markers reported to define effector and naïve cells. The one possible exception was with CD7 versus C1.7, where tetramer$^+$ cells were almost all high in expression of both markers (associated with cytotoxic T cells).

Coda

Maximization of signal over noise, running appropriate controls, determining the lower limit of detection, and acquisition of an appropriate number of events are the elements of successful rare-event detection. When dealing with multiparameter datasets, it is useful to think of parameters as classifiers or outcomes. This facilitates a hierarchic analysis that avoids the *all possible permutations* problem (ie, 112 distinct parameter combinations in the last example). Having done this, it is feasible and practical to perform functional, kinetic, and high-resolution immunophenotypic studies on well-defined populations that comprise only a small proportion of total cells within heterogeneous tissues.

Acknowledgments

The authors would like to thank Kit Snow, Tom Franks, Erin McClelland, E. Michael Meyer, Darlene Monlish, Linda Moore, Peter Nobes,

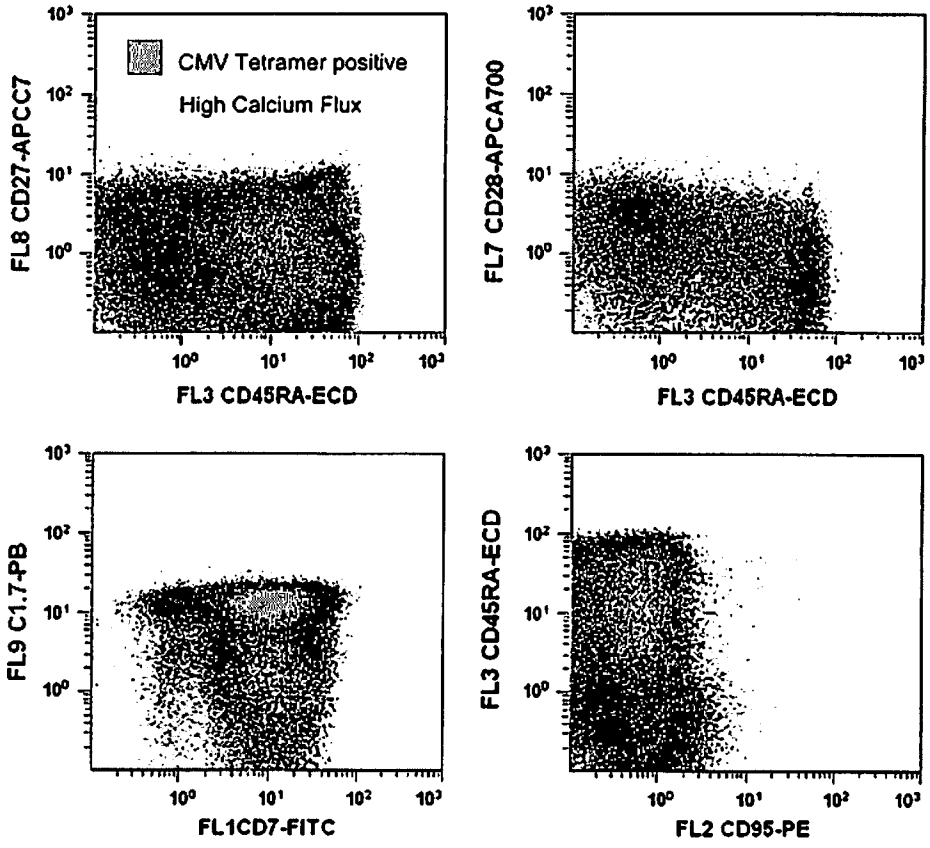

Fig. 15. Use of color eventing to examine relationships between classifier and outcome variables. All events were gated according to the primary classifier criteria (see text) and on the time segment before the addition of ionomycin. CMV tetramer+ events were color-evented red; cells with high calcium flux after tetramer addition were color-evented yellow, with color precedence going to the tetramer-positive (red) cells. Tetramer-negative, calcium flux–negative cells are blue.

Melanie Pfeiffer, and David Roberts for their assistance with various aspects of the original data presented here.

References

[1] Gross HJ, Verwer B, Houck D, et al. Model study detecting breast cancer cells in peripheral blood mononuclear cells at frequencies as low as 10(−7). Proc Natl Acad Sci U S A 1995; 92(2):537–41.

[2] van den Engh G. New applications of flow cytometry. Curr Opin Biotechnol 1993;4(1):63–8.

[3] Rosenblatt JI, Hokanson JA, McLaughlin SR, et al. Theoretical basis for sampling statistics useful for detecting and isolating rare cells using flow cytometry and cell sorting. Cytometry 1997;27(3):233–8.

[4] Donnenberg AD, Meyer EM. Principles of rare event analysis by flow cytometry: detection of injected dendritic cells in draining lymphatic tissue. Clinical Immunology Newsletter 1999; 19(10–11):124–8.

[5] Baumgarth N, Roederer M. A practical approach to multicolor flow cytometry for immunophenotyping. J Immunol Methods 2000;243(1–2):77–97.

[6] Donnenberg VS, Donnenberg AD. Identification, rare-event detection and analysis of dendritic cell subsets in broncho-alveolar lavage fluid and peripheral blood by flow cytometry. Front Biosci 2003;8:s1175–80.
[7] Altman JD, Moss PAH, Goulder PR, et al. Phenotypic analysis of antigen-specific T lymphocytes. Science 1996;274:94–6.
[8] NIH Tetramer Core Facility at Emory University. Available at: http://research.yerkes.emory.edu/tetramer_core/index.html. Accessed June 18, 2007.
[9] Maino VC, Picker LJ. Identification of functional subsets by flow cytometry: intracellular detection of cytokine expression. Cytometry 1998;34(5):207–15.
[10] Listman JA, Wang Y, Castro JE, et al. Detection of rare apoptotic T cells in vivo. Cytometry 1998;33(3):340–7.
[11] Muraro PA, Jacobsen M, Necker A, et al. Rapid identification of local T cell expansion in inflammatory organ diseases by flow cytometric T cell receptor Vbeta analysis. J Immunol Methods 2000;246(1–2):131–43.
[12] Walle AJ, Niedermayer W. Aneuploidy as a marker of minimal residual disease in leukemia. Cancer Detect Prev 1985;8(1–2):303–15.
[13] Ryan DH, Mitchell SJ, Hennessy LA, et al. Improved detection of rare CALLA-positive cells in peripheral blood using multiparameter flow cytometry. J Immunol Methods 1984; 74(1):115–28.
[14] Hussain M, Kukuruga M, Biggar S, et al. Prostate cancer: flow cytometric methods for detection of bone marrow micrometastases. Cytometry 1996;26(1):40–6.
[15] Balic M, Dandachi N, Hofmann G, et al. Comparison of two methods for enumerating circulating tumor cells in carcinoma patients. Cytometry B Clin Cytom 2005;68(1):25–30.
[16] Allard WJ, Matera J, Miller MC, et al. Tumor cells circulate in the peripheral blood of all major carcinomas but not in healthy subjects or patients with nonmalignant diseases. Clin Cancer Res 2004;10(20):6897–904.
[17] Dick JE. Breast cancer stem cells revealed. Proc Natl Acad Sci U S A 2003;100(7):3547–9.
[18] Donnenberg VS, Donnenberg AD. Multiple drug resistance in cancer revisited: the cancer stem cell hypothesis. J Clin Pharmacol 2005;45(8):872–7.
[19] Donnenberg VS, Luketich JD, Landreneau RJ, et al. Tumorigenic epithelial stem cells and their normal counterparts. Ernst Schering Res Found Workshop, in press.
[20] Donnenberg VS, Landreneau RJ, Donnenberg AD. Tumorigenic stem and progenitor cells: implications for the therapeutic index of anti-cancer agents. J Control Release, in press.
[21] Al-Hajj M, Wicha MS, Benito-Hernandez A, et al. Prospective identification of tumorigenic breast cancer cells. Proc Natl Acad Sci U S A 2003;100(7):3983–8.
[22] Singh SK, Hawkins C, Clarke ID, et al. Identification of human brain tumour initiating cells. Nature 2004;432(7015):396–401.
[23] Szotek PP, Pieretti-Vanmarcke R, Masiakos PT, et al. Ovarian cancer side population defines cells with stem cell-like characteristics and Mullerian Inhibiting Substance responsiveness. Proc Natl Acad Sci U S A 2006;103(30):11154–9.
[24] Goodell MA, Brose K, Paradis G, et al. Isolation and functional properties of murine hematopoietic stem cells that are replicating in vivo. J Exp Med 1996;183(4):1797–806.
[25] Zhou S, Schuetz JD, Bunting KD, et al. The ABC transporter Bcrp1/ABCG2 is expressed in a wide variety of stem cells and is a molecular determinant of the side-population phenotype. Nat Med 2001;7(9):1028–34.
[26] Muller C, Bonmann M, Cassens U, et al. Flow cytometric analysis of protein phosphorylation in the hematopoetic system. Leuk Lymphoma 1998;29(3–4):351–60.
[27] Rosu-Myles M, Khandaker M, Wu DM, et al. Characterization of chemokine receptors expressed in primitive blood cells during human hematopoietic ontogeny. Stem Cells 2000; 18(5):374–81.
[28] Henon PH, Sovalat H, Bourderont D. Importance of CD34+ cell subsets in autologous PBSC transplantation: the mulhouse experience using CD34+CD38- cells as predictive tool for hematopoietic engraftment. J Biol Regul Homeost Agents 2001;15(1):62–7.

[29] Pratt G, Rawstron AC, English AE, et al. Analysis of CD34+ cell subsets in stem cell harvests can more reliably predict rapidity and durability of engraftment than total CD34+ cell dose, but steady state levels do not correlate with bone marrow reserve. Br J Haematol 2001;114(4):937–43.
[30] Shapiro R, Rao AS, Fontes P, et al. Combined simultaneous kidney/bone marrow transplantation. Transplantation 1995;60(12):1421–5.
[31] Ribatti D. The discovery of endothelial progenitor cells. An historical review. Leuk Res 2007;31(4):439–44.
[32] Jones EA, English A, Kinsey SE, et al. Optimization of a flow cytometry-based protocol for detection and phenotypic characterization of multipotent mesenchymal stromal cells from human bone marrow. Cytometry B Clin Cytom 2006;70(6):391–9.
[33] George F, Brisson C, Poncelet P, et al. Rapid isolation of human endothelial cells from whole blood using S-Endo1 monoclonal antibody coupled to immuno-magnetic beads: demonstration of endothelial injury after angioplasty. Thromb Haemost 1992;67(1): 147–53.
[34] Bohmer RM, Zhen D, Bianchi DW. Identification of fetal nucleated red cells in co-cultures from fetal and adult peripheral blood: differential effects of serum on fetal and adult erythropoiesis. Prenat Diagn 1999;19(7):628–36.
[35] Geifman-Holtzman O, Makhlouf F, Kaufman L, et al. The clinical utility of fetal cell sorting to determine prenatally fetal E/e or e/e Rh genotype from peripheral maternal blood. Am J Obstet Gynecol 2000;183(2):462–8.
[36] Bajaj S, Welsh JB, Leif RC, et al. Ultra-rare-event detection performance of a custom scanning cytometer on a model preparation of fetal nRBCs. Cytometry 2000;39(4): 285–94.
[37] Bianchi DW, Zickwolf GK, Weil GJ, et al. Male fetal progenitor cells persist in maternal blood for as long as 27 years postpartum. Proc Natl Acad Sci U S A 1996;93(2):705–8.
[38] Qu L, Triulzi DJ, Rowe DT, et al. Stability of Lymphocytes and EBV during RBC Storage. Vox Sanguinis 2007;92:125–9.
[39] Garritsen HS, Sibrowski W. Flow cytometric determination of leukocytes and lymphocyte subsets in thrombocytapheresis products. Beitr Infusionsther Transfusionsmed 1994;32: 401–4.
[40] Triulzi DJ, Meyer EM, Donnenberg AD. WBC subset analysis of WBC-reduced platelet components. Transfusion 2000;40(7):771–80.
[41] Barrat-Boyes SM, Zimmer MI, Harshyne LA, et al. Maturation and trafficking of monocyte-derived dendritic cells in monkeys: implications for dendritic cell-based vaccines. J Immunol 2000;164:2487–95.
[42] Parish CR. Fluorescent dyes for lymphocyte migration and proliferation studies. Immunol Cell Biol 1999;77(6):499–508.
[43] Donnenberg VS, O'Connell PJ, Logar AJ, et al. Rare event analysis of circulating human dendritic cell subsets and their presumptive mouse counterparts. Transplantation 2001; 72(12):1946–51.
[44] McIlroy D, Troadec C, Grassi F, et al. Investigation of human spleen dendritic cell phenotype and distribution reveals evidence of in vivo activation in a subset of organ donors. Blood 2001;97(11):3470–7.
[45] Morelli AE, Hackstein H, Thomson AW. Potential of tolerogenic dendritic cells for transplantation. Semin Immunol 2001;13(5):323–35.
[46] Fong L, Brockstedt D, Benike C, et al. Dendritic cells injected via different routes induce immunity in cancer patients. J Immunol 2001;166(6):4254–9.
[47] Kuwana M, Kaburaki J, Wright TM, et al. Induction of antigen-specific human CD4(+) T cell anergy by peripheral blood DC2 precursors. Eur J Immunol 2001;31(9):2547–57.
[48] Liau S, Yancovitz SR, Qureshi MN, et al. The number of CD1a+ large low-density cells with dendritic cell features is increased in the peripheral blood of HIV+ patients. Clin Immunol Immunopathol 1994;70(3):190–7.

[49] Kramer B, Grobusch MP, Suttorp N, et al. Relative frequency of malaria pigment-carrying monocytes of nonimmune and semi-immune patients from flow cytometric depolarized side scatter. Cytometry 2001;45(2):133–40.
[50] Medina F, Segundo C, Brieva JA. Purification of human tonsil plasma cells: pre-enrichment step by immunomagnetic selection of CD31(+) cells. Cytometry 2000;39(3):231–4.
[51] Rehse MA, Corpuz S, Heimfeld S, et al. Use of fluorescence threshold triggering and high-speed flow cytometry for rare event detection. Cytometry 1995;22(4):317–22.
[52] Shapiro HM. Practical flow cytometry. 4th edition. Hoboken (NJ): John Wiley and Sons; 2003.
[53] Cupp JE, Leary JF, Cernichiari E, et al. Rare-event analysis methods for detection of fetal red blood cells in maternal blood. Cytometry 1984;5(2):138–44.
[54] Owens M, Loken MR. Flow cytometry principles for clinical laboratory practice: quality assurance for quantitative immunophenotyping. New York: Wylie-Liss; 1995. p. 111–28.
[55] Aubin JE. Autofluorescence of viable cultured mammalian cells. J Histochem Cytochem 1979;27(1):36–43.
[56] Hoffmann TK, Donnenberg VS, Friebe-Hoffmann U, et al. Rapid communication: competition of peptide-MHC class I tetrameric complexes with anti-CD3 provides evidence for specificity of peptide binding to the tcr complex. Cytometry 2000;41:321–8.
[57] Telford W, Murga M, Hawley T, et al. DPSS yellow-green 561-nm lasers for improved fluorochrome detection by flow cytometry. Cytometry A 2005;68(1):36–44.
[58] Gross HJ, Verwer B, Houck D, et al. Detection of rare cells at a frequency of one per million by flow cytometry. Cytometry 1993;14(5):519–26.
[59] Roederer M. Spectral compensation for flow cytometry: visualization artifacts, limitations, and caveats. Cytometry 2001;45(3):194–205.
[60] Sutherland DR, Anderson L, Keeney M, et al. The ISHAGE guidelines for CD34+ cell determination by flow cytometry. International Society of Hematotherapy and Graft Engineering. J Hematother 1996;5(3):213–26.
[61] June CH, Ledbetter JA, Rabinovitch PS, et al. Distinct patterns of transmembrane calcium flux and intracellular calcium mobilization after differentiation antigen cluster 2 (E rosette receptor) or 3 (T3) stimulation of human lymphocytes. J Clin Invest 1986;77(4):1224–32.